



Isolation, Structure Determination, and Cytotoxic Activity of Steroid Compound from The Stem Bark of *Aglaiacucullata* (Meliaceae)

Kindi Farabi^{a,*}, Desi Harneti^a, Nurlelasari^a, Tri Mayanti^a, Rani Maharani^a,
 Unang Supratman^{a,b}



^a Department of Chemistry, Faculty of Mathematics and Natural Sciences, Universitas Padjadjaran, Jatinangor 45363, Indonesia

^b Central Laboratory, Universitas Padjadjaran, Jatinangor 45363, Indonesia

* Corresponding author: kindi.farabi@unpad.ac.id

<https://doi.org/10.14710/jksa.26.6.217-223>

Article Info

Article history:

Received: 12th July 2023

Revised: 30th August 2023

Accepted: 31st August 2023

Online: 30th September 2023

Keywords:

Steroid; *Aglaiacucullata*;
 cytotoxic activity

Abstract

Steroids are one of the secondary metabolite groups that are abundant in many organisms. In plants, this type of compound is called phytosterols. Phytosterols have been widely known to show many potential bioactivities such as anti-inflammatory, induced apoptosis, cytotoxic, anti-diabetic, angiogenic, and antioxidant. One of the sources of phytosterol compounds is the genus *Aglaiacucullata*. As the largest genus in the Meliaceae family, the genus *Aglaiacucullata* contains many bioactive compounds, including steroids. This research reported the isolation, structural determination, and cytotoxic activity of steroid compounds from the stem bark of *Aglaiacucullata*, one of the members of the *Aglaiacucullata* genus. Pure isolated steroid was obtained after maceration of dried stem bark with ethanol and partitioned based on difference polarity, continued by column chromatography. Spectroscopic methods, including HRMS, FTIR, 1D and 2D NMR, were used for structural determination. The compound structure identified as stigmast-5-en-3 β -ol-3 β -oleate was first isolated from this species. MCF-7 breast cancer cell, B16-F10 melanoma cell, and CV-1 normal fibroblast kidney cell were used to evaluate its cytotoxicity. Stigmast-5-en-3 β -ol-3 β -oleate displayed low cytotoxicity against those two cancer cells and a normal cell.

1. Introduction

Steroids are derived from modified triterpenoids containing a tetracyclic ring system, with the loss of three methyl groups at C-4 and C-14 [1]. Its main skeleton consists of four rings: one five-membered cyclic and three six-membered cyclic [2]. Steroids are widely found in many organisms, such as fungi, plants, and animals, and show structural features similar to cholesterol [3]. Steroid compounds, especially those usually found in plants, sitosterol, showed remarkably diverse biological activity, such as inducing apoptosis [4], angiogenic [5], anti-inflammation [6], anti-diabetic [7], anti-oxidant [8], and hypocholesterolemic [9].

Aglaiacucullata is a genus in the Meliaceae family, which is also the largest genus in this family, widely distributed in the tropical rain forests of Southeast Asia, including Indonesia and Malaysia [10]. *Aglaiacucullata* plants are known to contain various secondary metabolites with interesting

biological activities like anticancer, anti-inflammatory, antioxidant, antimicrobial, and antidiabetic [11]. Phytochemical studies in the genus *Aglaiacucullata* indicated the content of various secondary metabolites such as roscaglamide, triterpenoids, diterpenoids, sesquiterpenoids, limonoids, steroids, lignans, and alkaloids [11]. Traditionally, this plant has been used to treat various ailments such as cancer, heart problems, fever, inflammation, and coughs [12].

Aglaiacucullata is a unique species of *Aglaiacucullata* that grows only in mangrove ecosystems [13]. Traditionally, this plant is utilized for house structure [14]. This plant extract was used in the medicinal field to treat dysentery, skin infection, diarrhea, and heart problems [15]. Previous chemical component investigations of these plants revealed the presence of cytotoxic compounds against human cancer cell lines [16].

This research aims to isolate steroid compound from the stem bark of *A. cucullata* using extractions, separations, and purification methods such as maceration, partitioned, and column chromatography, followed by identification of its chemical structure using various spectroscopic methods to give a known stigmastane steroid (**1**). The previous study from this species revealed no reported isolation of steroid compounds. Thus, this study presented for the first time the isolation and structure determination of steroid compounds together with cytotoxic activity tested against MCF-7 breast cancer, B16-F10 melanoma, and CV-1 normal kidney fibroblast cell lines. The cytotoxicity of compound **1** against those cancer cells was also reported for the first time.

2. Experimental

This research started with the sampling of stem bark of *A. cucullata*. After drying and grinding, the crushed stem bark of *A. cucullata* was macerated with ethanol (EtOH), filtered, and evaporated under reduced pressure. EtOH extract was then partitioned with *n*-hexane, ethyl acetate (EtOAc), and *n*-butanol (*n*-BuOH). Separation and purification of *n*-hexane extract using chromatographic methods were then performed to produce pure compound **1**. Spectroscopic methods were utilized to determine its chemical structure. After the chemical structure was confirmed, a bioassay was carried out against MCF-7 breast cancer, B16-F10 melanoma, and CV-1 normal kidney fibroblast cell lines. The resulting cytotoxicity tested was in IC₅₀ and then compared with positive control (cisplatin).

2.1. General Experimental Procedures

The high-resolution mass spectra (HRESI-TOFMS) were obtained on a Waters Xevo Q-TOF direct probe/MS system using ESI⁺ mode and microchannel plates MCPs detector (Milford, MA, USA). The IR spectra were measured on a One Perkin Elmer infrared-100 (Shelton, Connecticut, USA). The measurement of HRMS and FTIR were conducted in Laboratorium Sentral (Central Laboratory), Universitas Padjadjaran, Sumedang, Indonesia. The NMR data were recorded on a JEOL ECZ-500 spectrometer (Tokyo, Japan) at 500 MHz for ¹H and 125 MHz for ¹³C using TMS as an internal standard and CDCl₃ as a solvent. The NMR measurement was carried out at Badan Riset dan Inovasi Nasional (BRIN), Serpong, South Tangerang, Indonesia. Chromatographic separations were conducted on a silica gel G60 (Merck, Darmstadt, Germany, 70–230 and 230–400 mesh). The TLC plates were precoated with GF₂₅₄ (Merck, 0.25 mm), after which detection was performed by spraying with 10% H₂SO₄ in ethanol before heating.

The equipment used in this study included glassware commonly used in organic chemistry laboratories. Concentration of macerate and fractions was carried out using a rotary evaporator type R-215 Buchi equipped with a V-700 vacuum pump, B-491 water bath, and F-100 cold circulator. Compounds were separated using different sizes of open column chromatography (diameters: 1, 1.5, 2, and 2.5 cm with 50 cm in height).

2.2. Plant Material

The stem bark of *A. cucullata* was obtained from the Manggar River in Balikpapan, East Kalimantan, Indonesia (1°11'25" S, 116°57'29" E). This sample was classified by the staff of the Herbarium Wanariset, Balikpapan, in December 2020, and the specimen was deposited at the herbarium (collection No. FF7.20).

2.3. Extraction and Isolation

The crushed dried stem bark of *A. cucullata* (3.5 kg) was extracted with ethanol (5 x 3 L) at room temperature for five days. After solvent evaporation, 523 g extract was obtained and partitioned based on different polarity to give 64 g, 35 g, and 13 g of the *n*-hexane, ethyl acetate, and 1-butanol extract, respectively.

A total of 64 g of the *n*-hexane extract was fractionated by vacuum liquid chromatography (r: 5 cm; h: 12 cm) on silica gel (300 g of G60 silica gel) using a gradient elution of *n*-hexane-ethyl acetate (10:0–0:10, stepwise 10%; v: 500 mL) continued by ethyl acetate-methanol (10:0–0:10, stepwise 10%; v: 500 mL) to give eight fractions (A–H). Subsequently, 21 g of B was separated by vacuum liquid chromatography (r: 5 cm; h: 12 cm) on silica gel (200 g of G60 silica gel) using a gradient elution of *n*-hexane-ethyl acetate (10:0–0:10, stepwise 5%; v: 300 mL) to give six fractions (B1–B6). A total of 2.7 g B1 was separated with silica gel column chromatography (70–230 mesh, 80 g) using a gradient elution of *n*-hexane-methylene chloride (10:0–1:1 stepwise 2.5%; r: 2 cm; h: 17 cm; v: 250 mL) to produce nine fractions (B1a–B1i). A total of 793 mg of fraction B1a was separated with silica gel column chromatography (230–400 mesh, 55 g) using a gradient elution of *n*-hexane-methylene chloride (10:0–9:1 stepwise 1%; r: 1 cm; h: 20 cm; v: 80 mL) to produce 74.3 mg of compound **1**.

2.4. Determination of Cytotoxic Activity

The cytotoxic bioassay was conducted using the PrestoBlue assay. Cell viability was assessed with Presto Blue reagent (Thermo Fisher Scientific, Uppsala, Sweden) to evaluate various resazurin-based cell types viability rapidly and quantitatively proliferation using live-cell reduction capabilities. When cells are alive and healthy, they maintain a reduced environment in their cytosol. Reducing resazurin (blue) is a cell viability indicator using absorbance or fluorescent outputs to reduce resorufin (purple). The conversion is proportional to the number of metabolically active cells. Briefly, MCF-7 cell lines, B16-F10, and CV-1 cell lines were grown in 70% confluent harvested and counted, then diluted with complete culture RPMI medium. The cells were then transferred into 96-well plates with 170,000 cells/well. After overnight growth, the cells were treated with increasing concentrations of compound **1** (3.91, 7.81, 15.63, 31.25, 62.50, 125, 250, 5,000 µg/mL) with co-solvent 2% (v/v) DMSO in PBS. Cisplatin was used as the positive control. All samples were incubated at 37°C in a 5% CO₂ incubator for 24 h. After incubation, the medium was immediately replaced by 10 µL PrestoBlue reagent in a 90 µL RPMI medium. The plates were incubated for 1 to 2 h until

resorufin was formed (color changes from blue to purple). The absorbance was measured at 570 nm using a microplate reader. The IC₅₀ value is the concentration for 50% growth inhibition. The percentage of cytotoxicity compared to untreated cells was determined. A plot of % cytotoxicity versus sample concentrations was used to calculate the concentration, which showed 50% cytotoxicity (IC₅₀). All assays and analyses were run in duplicate, and all were averaged.

3. Results and Discussion

About 3.5 kg of dried, crushed stem bark of *A. cucullata* was macerated using EtOH. Ethanol was considered a safe solvent in terms of health for extracting compounds from nature [17]. This stem bark of *A. cucullata* was obtained from the Manggar River in East Kalimantan because this is the native habitat of this plant. After evaporating at reduced pressure, 525 g of brown thick ethanol extract was obtained (15% of the initial

weight of the sample). This extract was very complex, with many compounds observed in a thin-layer chromatography plate. Therefore, the partition based on different polarity was carried out, namely with *n*-hexane (64 g), ethyl acetate (35 g), and 1-butanol (13 g).

Phytochemical tests in thin-layer chromatography plates showed that *n*-hexane extract contained purple to red color spots after sprayed with 10% H₂SO₄ in ethanol, indicating the presence of steroid compounds. The other extract (ethyl acetate and 1-butanol) did not show any positive result of the steroid compound, so the separation and purification were focused on *n*-hexane extract. Since *n*-hexane extract was in large quantities (more than 20 g), vacuum liquid chromatography was used for the first separation methods, followed by several steps of column chromatography guided by thin-layer chromatography. Compound 1 was obtained in a pure form.

Table 1. NMR data of compound 1 (500 MHz for ¹H and 125 MHz for ¹³C in CDCl₃) [18]

Position	¹³ C-NMR δ _c (mult.)	¹ H-NMR δ _H (Integral, mult., J=Hz)	Position	¹³ C-NMR δ _c (mult.)	¹ H-NMR δ _H (Integral, mult., J=Hz)
1	37.1 (t)	1.86 (2H, m)	1'	173.4 (s)	-
2	32.0 (t)	1.96 (2H, m)	2'	34.8 (t)	2.25 (2H, t, 7.8)
3	73.7 (d)	4.58 (1H, m)	3'	25.5 (t)	1.59 (2H, m)
4	39.8 (t)	1.98 (2H, m)	4'	29.2 (t)	1.29 (2H, m)
5	139.8 (s)	-	5'	29.6 (t)	1.24 (2H, m)
6	122.7 (d)	5.34 (1H, s)	6'	29.4 (t)	1.24 (2H, m)
7	32.1 (t)	1.92 (2H, m)	7'	29.8 (t)	1.24 (2H, m)
8	31.8 (d)	1.48 (1H, m)	8'	27.2 (t)	1.98 (2H, m)
9	50.1 (d)	0.92 (1H, m)	9'	129.9 (d)	5.33 (1H, dd, 3.1, 9.6)
10	36.6 (s)	-	10'	130.1 (d)	5.33 (1H, dd, 3.1, 9.6)
11	21.0 (t)	1.46 (2H, m)	11'	27.3 (t)	1.98 (2H, m)
12	38.2 (t)	2.28 (2H, m)	12'	29.9 (t)	1.24 (2H, m)
13	42.4 (s)	-	13'	29.5 (t)	1.24 (2H, m)
14	56.7 (d)	0.99 (1H, m)	14'	29.7 (t)	1.24 (2H, m)
15	24.4 (t)	0.97 (2H, m)	15'	29.3 (t)	1.29 (2H, m)
16	28.2 (t)	1.82 (2H, m)	16'	27.9 (t)	1.85 (2H, m)
17	56.1 (d)	1.06 (1H, m)	17'	22.8 (t)	1.27 (2H, m)
18	11.8 (q)	0.64 (3H, s)	18'	14.2 (q)	0.86 (3H, t, 6.6)
19	19.3 (q)	1.00 (3H, s)			
20	36.2 (d)	1.30 (1H, m)			
21	18.9 (q)	0.91 (3H, d, 3.5)			
22	33.9 (t)	1.22 (2H, m)			
23	26.0 (t)	1.14 (2H, m)			
24	45.9 (d)	0.92 (1H, m)			
25	29.1 (d)	1.28 (2H, m)			
26	19.9 (q)	0.84 (3H, d, 6.5)			
27	19.0 (q)	0.82 (3H, d, 6.5)			
28	23.1 (t)	1.24 (2H, m)			
29	12.2 (q)	0.83 (3H, t, 1.7)			

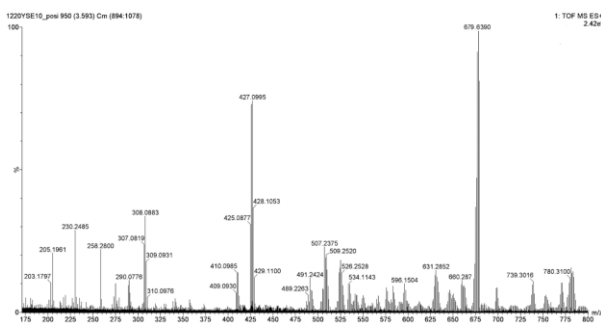


Figure 1. HRMS spectrum of compound 1 [18]

Compound 1 was in a white amorphous powder form. The chemical formula of compound 1, determined as $C_{47}H_{82}O_2$ based on HRMS data, showed an $[M+H]^+$ ion peak at m/z 679.6390 (calcd. 679.6393 for $C_{47}H_{83}O_2$) (Figure 1) together with 1H NMR and ^{13}C NMR spectra data (Table 1). The FTIR measurement (Figure 2) resulted that in compound 1 existed stretching of C-H sp^3 (2982 cm^{-1}), stretching of C=O (1737 cm^{-1}), stretching of C=C (1606 cm^{-1}), bending of C-H *gem*-dimethyl (1460 and 1352 cm^{-1}), and stretching of C-O (1054 cm^{-1}) [18].

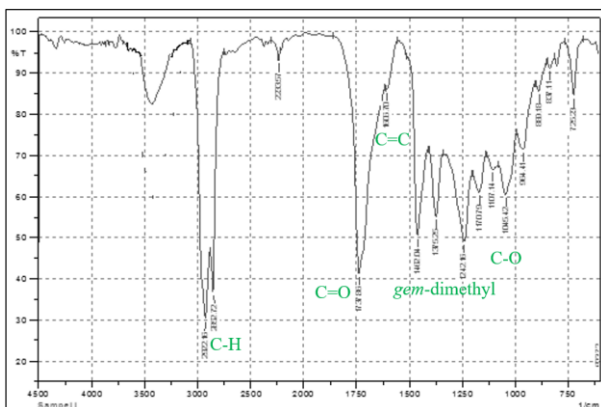


Figure 2. FTIR spectrum of compound 1 [18]

The 1H NMR spectrum of compound 1 (Figure 3) showed the presence of seven methyls, including two tertiary methyls at δ_H 0.64 (3H, s) and 1.00 (3H, s), three secondary methyls at δ_H 0.82 (3H, d, $J=6.5\text{ Hz}$), 0.84 (3H, d, $J=6.5\text{ Hz}$), and 0.91 (3H, d, $J=3.5\text{ Hz}$), and two primary methyls at δ_H 0.83 (3H, t, $J=1.7\text{ Hz}$) and 0.86 (3H, t, $J=6.6\text{ Hz}$). The signal characteristic for oxygenated methine was also observed at δ_H 4.58 (1H, m) and the olefinic group at δ_H 5.33 (2H, dd, $J=3.1$, and 9.6 Hz), which is suitable for *cis*-conformation [18] and δ_H 5.34 (1H, s). The specific signal for the substituent of fatty acid was also clearly seen at 1H 1.24 with high integrity, indicating the presence of an overlapping signal [19, 20]. Other 1H NMR peaks were overlapping and could be assigned perfectly using two-dimensional NMR, especially HMQC experiments with ^{13}C NMR.

The ^{13}C NMR spectrum detailed by DEPT 135° (Figure 3) proved the presence of 47 carbon signals, including seven methyls, 25 methylenes, eleven methines (including one oxymethine at δ_H 73.7 and three sp^2

methine at δ_H 122.7, 129.9, and 130.1), and four quaternary carbons (including one quaternary olefinic at δ_H 139.8 and one carbonyl ester at δ_H 173.4). Based on 1H NMR, ^{13}C NMR, and DEPT 135° spectra, it can be concluded that the structure of compound 1 consists of one ester group, two double bonds, a fatty acid substituent, and a stigmastane-type steroid. However, to determine the exact position of each functional group, a two-dimensional NMR experiment (HMQC, HMBC, and 1H - 1H COSY) was necessary.

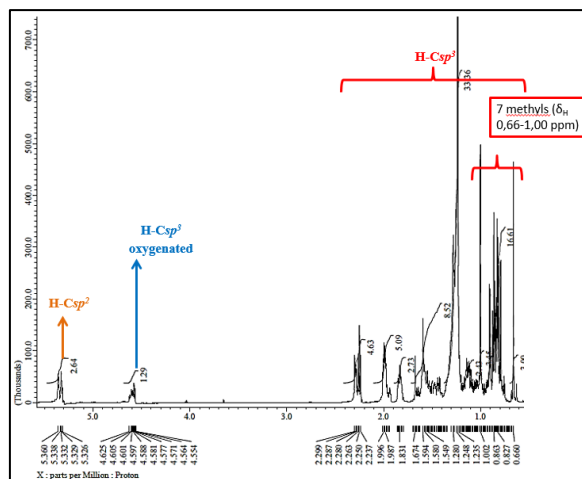


Figure 3. 1H NMR spectrum of compound 1 (500 MHz in $CDCl_3$) [18]

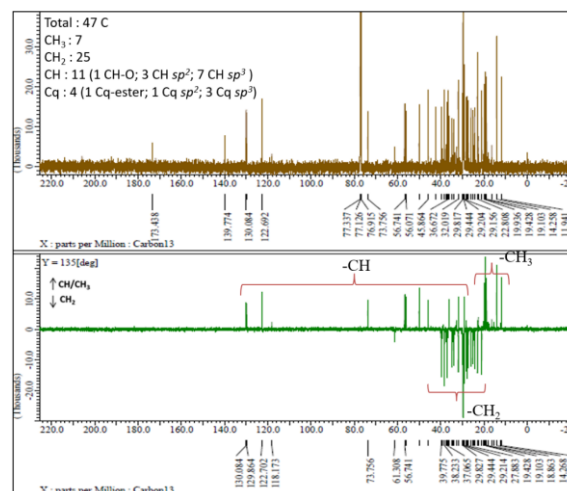


Figure 4. ^{13}C NMR spectrum of compound 1 (125 MHz in $CDCl_3$) [18]

HMQC (Heteronuclear Multiple Quantum Coherence) experiments were used to determine the correlation of proton (hydrogen) with carbon in one bond. On the other hand, with this correlation, the pairing of each hydrogen and carbon can be determined [21]. The NMR table (Table 1) at each position is determined by the HMQC experiments. However, HMBC (Heteronuclear Multiple Bond Correlation) was utilized to determine the exact position of each functional group because this type of spectrum will correlate proton (hydrogen) and carbon in two or three-bond distances.

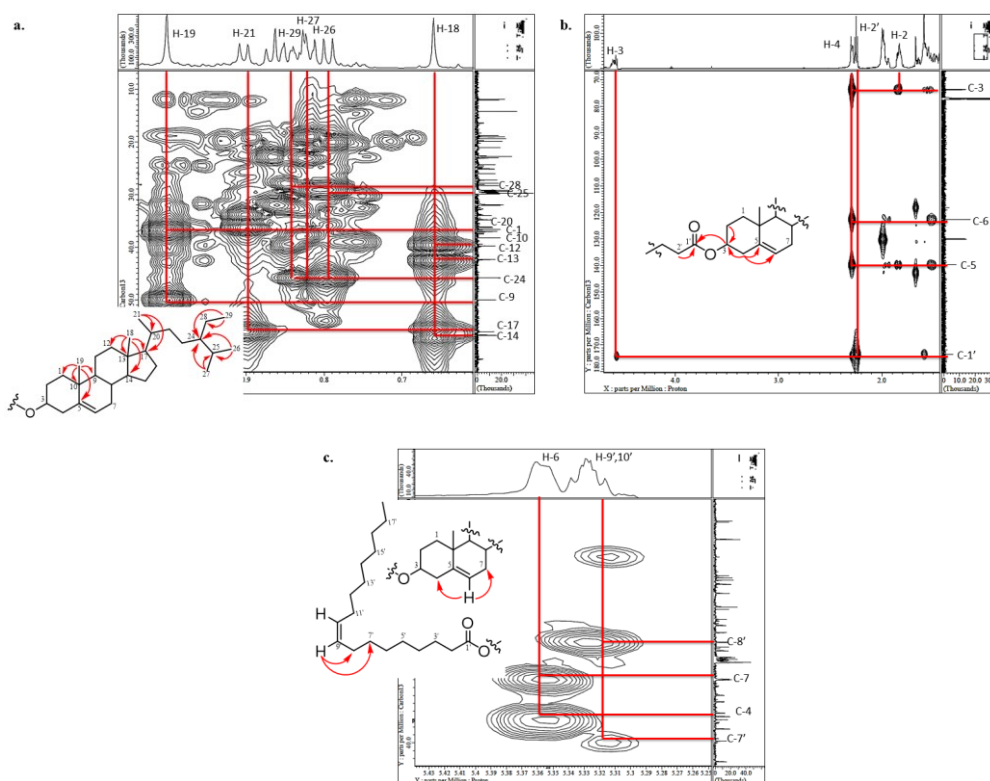


Figure 5. HMBC spectrum of compound 1: a) The attachment of each methyl group in compound 1, b) The position of double bond and fatty acid ester substituent attachment, c) The position of the double bond in the fatty acid ester chain [18]

HMBC of compound 1 is shown in Figure 5. Figure 5a shows the attachment of each methyl group in compound 1. Correlation arising from H-19 to C-1, C-10, C-5, and C-9, and correlations of H-18 to C-12, C-13, C-14, C-17 determined the tetracyclic core of this compound. Correlations observed at H-21 to C-17 and C-20 and correlations of H-29 to C-28 and C-24, and correlation observed at H-26 and H-27 to C-25 and C-24, used for the determination of the side chain of compound 1. Thus, those correlations determined the main skeleton of compound 1 as a stigmastane-type steroid. The position of double bond at C-5/C-6 was determined by the HMBC correlations of H-4 to C-5 and C-6. The oxymethine that appears at C-3 resulted from

the correlations of H-2 and H-4 to C-3, together with the attachment of the ester group at C-3 by the correlations of H-3 to C-1' and H-2' to C-1' (Figure 5b). Another double bond at C-9'/C-10' was confirmed based on correlations of H-9' to C-8' and C-7' (Figure 5c).

¹H-¹H COSY (Correlated Spectroscopy) is based on the cross-peak of protons (hydrogens) in three distances, so this type of correlation will confirm the position of neighboring hydrogens. Crosspeak observed at H-2/H-3/H-4 confirmed that oxymethine attached at the C-3 position. A double bond at C-5/C-6 was observed based on the cross-peak of H-6/H-7. Other cross-peak correlations are also detailed in Figure 6.

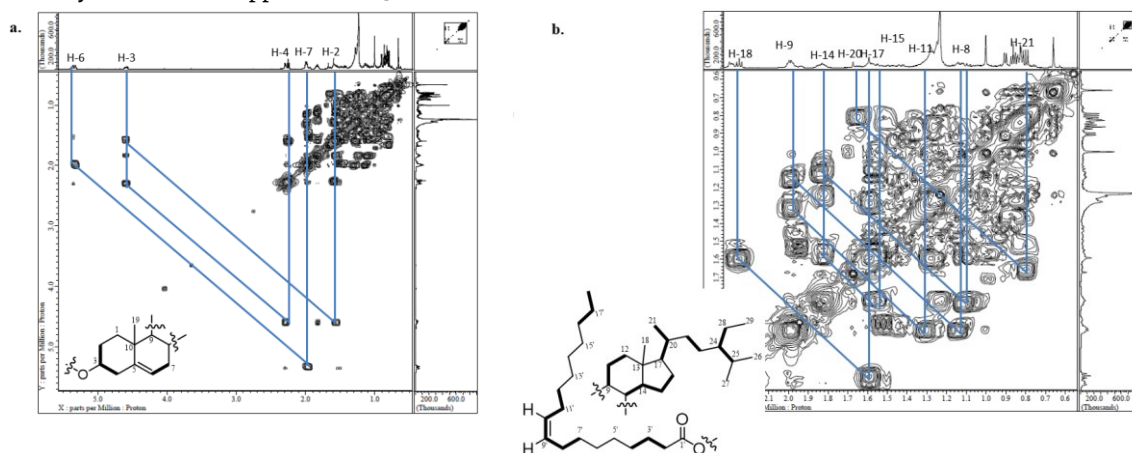


Figure 6. ¹H-¹H COSY spectrum of compound 1: a. COSY spectrum of ring A and B, b. COSY spectrum of ring C, D, side chain, and fatty acid ester substituent [18]

The results of ^1H , ^{13}C , HMQC, HMBC, and ^1H - ^1H COSY NMR analysis unambiguously determined the planar structure of compound **1** (Figure 7). However, the stereochemistry of compound **1** has not been identified. The best way to determine the stereochemistry of compound **1** is with the comparison of its NMR data, including its coupling constant (J) in ^1H NMR and the biogenetic approach of stigmastane-type steroids, especially with previous compounds found in the *Aglaia* genus. Thus, based on a comparison with previous literature [18], compound **1** was identified as a stigmastane-type steroid, namely, 3β -sitosteryl-oleate (Figure 8), which was isolated for the first time in this species. This compound can be classified as a nonpolar compound since this compound contains many hydrocarbon chains, for example, the fatty acid ester substituent and side chain in the main skeleton. This result is consistent with the appearance of this compound in *n*-hexane extract, which is the most nonpolar extract among all extracts.

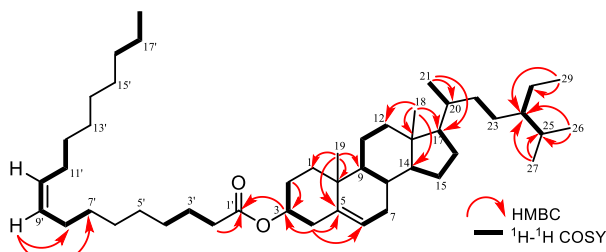


Figure 7. Total HMBC and ^1H - ^1H COSY correlations of compound **1**

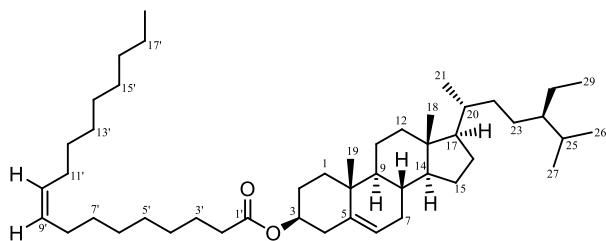


Figure 8. Chemical structure of compound **1**

Compound **1** was tested against two cancer cells (MCF-7 breast cancer cell lines and B16-F10 melanoma cell lines) and a normal cell (CV-1 kidney fibroblast cell). The results of the Prestoblue cell anti-proliferation assay showed that IC_{50} value with cisplatin acts as a positive control ($\text{IC}_{50} = 53.00, 43.00, \text{ and } 43.00 \mu\text{M}$, respectively, for MCF-7, B16-F10, and CV-1). Unfortunately, compound **1** performed very weak cytotoxic activity with $\text{IC}_{50} > 300 \mu\text{M}$ for all tested cells (MCF-7, B16-F10, and CV-1). This result might be influenced by the presence of a fatty acid side chain, dramatically decreasing cytotoxic activity. In a previous study [12], it is clear that the appearance of fatty acid ester substituent in dammarane-type triterpenoid decreases cytotoxic activity against MCF-7, B16-F10. This fact may correlate with how weak compound **1** is against those cancer cell lines since the triterpenoids and steroids share similar chemical structures. The previous research [18] also revealed that 3β -sitosteryl-oleate performed weak cytotoxic activity against P-388 murine leukemia cells.

4. Conclusion

One stigmastane-type steroid compound has been successfully isolated from the stem bark of *A. cucullata* using various chromatography methods. The chemical structure of compound **1** has been determined utilizing spectroscopy data (^1H , ^{13}C , HMQC, HMBC, and ^1H - ^1H COSY NMR) and identified as 3β -sitosteryl-oleate. The cytotoxic assay against MCF-7 breast cancer cell lines, B16-F10 melanoma cell lines, and CV-1 normal kidney fibroblast cells were also performed. Compound **1** showed weak cytotoxic activity against all tested cells with $\text{IC}_{50} > 300 \mu\text{M}$.

Acknowledgment

This study was funded by Universitas Padjadjaran under the Head Lecturer Acceleration Research Grant with No. 2203/UN6.3.1/PT.00/2023 by Kindi Farabi and Academic Leadership Grant with No: 1959/UN6.3.1/PT.00/2023 by Unang Supratman.

References

- [1] Francesco Di Gioia, Spyridon A. Petropoulos, Phytoestrogens, phytosteroids and saponins in vegetables: Biosynthesis, functions, health effects and practical applications, in: *Advances in Food and Nutrition Research*, Elsevier, 2019, <https://doi.org/10.1016/bs.afnr.2019.02.004>
- [2] Ronda F. Greaves, Ganesh Jevalikar, Jacqueline K. Hewitt, Margaret R. Zacharin, A guide to understanding the steroid pathway: new insights and diagnostic implications, *Clinical Biochemistry*, 47, 15, (2014), 5-15 <https://doi.org/10.1016/j.clinbiochem.2014.07.017>
- [3] Soodabeh Saeidnia, Azadeh Manayi, Ahmad R. Gohari, Mohammad Abdollahi, The Story of Beta-sitosterol- A Review, *European Journal of Medicinal Plants*, 4, 5, (2014), 590-609 <https://doi.org/10.9734/EJMP/2014/7764>
- [4] Tamilselvam Rajavel, Pandian Packiyaraj, Venkatesan Suryanarayanan, Sanjeev Kumar Singh, Kandasamy Ruckmani, Kasi Pandima Devi, β -Sitosterol targets Trx/Trx1 reductase to induce apoptosis in A549 cells via ROS mediated mitochondrial dysregulation and p53 activation, *Scientific Reports*, 8, (2018), 2071 <https://doi.org/10.1038/s41598-018-20311-6>
- [5] Kai Qian, Xue-Xia Zheng, Chen Wang, Wen-Guang Huang, Xiao-Bao Liu, Shu-Di Xu, Dan-Kai Liu, Min-Ying Liu, Chang-Song Lin, β -Sitosterol inhibits rheumatoid synovial angiogenesis through suppressing VEGF signaling pathway, *Frontiers in Pharmacology*, 12, (2022), 816477 <https://doi.org/10.3389/fphar.2021.816477>
- [6] Pei-Chun Liao, Ming-Hoang Lai, Kuang-Ping Hsu, Yueh-Hsiung Kuo, Jie Chen, Ming-Chih Tsai, Chun-Xiang Li, Xi-Jiang Yin, Narumon Jeyashoke, Louis Kuo-Ping Chao, Identification of β -sitosterol as in vitro anti-inflammatory constituent in *Moringa oleifera*, *Journal of Agricultural and Food Chemistry*, 66, 41, (2018), 10748-10759 <https://doi.org/10.1021/acs.jafc.8b04555>
- [7] M. K. Radika, P. Viswanathan, C. V. Anuradha, Nitric oxide mediates the insulin sensitizing effects of β -sitosterol in high fat diet-fed rats, *Nitric Oxide*, 32,

- (2013), 43–53
<https://doi.org/10.1016/j.niox.2013.04.007>
- [8] Peng Zhang, Naicheng Liu, Mingyang Xue, Mengjie Zhang, Wei Liu, Chen Xu, Yuding Fan, Yan Meng, Qinghua Zhang, Yong Zhou, Anti-Inflammatory and Antioxidant Properties of β -Sitosterol in Copper Sulfate-Induced Inflammation in Zebrafish (*Danio rerio*), *Antioxidants*, 12, 2, (2023), 391
<https://doi.org/10.3390/antiox12020391>
- [9] Bahare Salehi, Cristina Quispe, Javad Sharifi-Rad, Natalia Cruz-Martins, Manisha Nigam, Abhay Prakash Mishra, Dmitry Alexeevich Kononov, Valeriya Orobinskaya, Ibrahim M. Abu-Reidah, Wissam Zam, Farukh Sharopov, Tommaso Venneri, Raffaele Capasso, Wirginia Kukula-Koch, Anna Wawruszak, Wojciech Koch, Phytosterols: From preclinical evidence to potential clinical applications, *Frontiers in Pharmacology*, 11, (2021), 1819
<https://doi.org/10.3389/fphar.2020.599959>
- [10] R. Priya, P. Sowmiya, M. S. Muthuraman, An overview on the biological perspectives of *Aglaia* species, *Asian Journal of Pharmaceutical and Clinical Research*, 11, 9, (2018), 42–45
<https://doi.org/10.22159/ajpcr.2018.v11i9.26436>
- [11] Desi Harneti, Unang Supratman, Phytochemistry and biological activities of *Aglaia* species, *Phytochemistry*, 181, (2021), 112540
<https://doi.org/10.1016/j.phytochem.2020.112540>
- [12] Kindi Farabi, Desi Harneti, Darwati, Tri Mayanti, Nurlelasari, Rani Maharani, Aprilia Permata Sari, Tati Herlina, Ace Tatang Hidayat, Unang Supratman, Sofa Fajriah, Mohamad Nurul Azmi, Yoshihito Shiono, Dammarane-Type Triterpenoid from the Stem Bark of *Aglaia elliptica* (Meliaceae) and Its Cytotoxic Activities, *Molecules*, 27, 19, (2022), 6757
<https://doi.org/10.3390/molecules27196757>
- [13] Wijarn Meepol, Gordon S. Maxwell, Sonjai Havanond, *Aglaia cucullata*: A little-known mangrove with big potential for research, *ISME/GLOMIS Electron Journal*, 18, 1, (2020), 4–9
- [14] Firoj Ahmed, Kazufumi Toume, Samir K. Sadhu, Takashi Ohtsuki, Midori A. Arai, Masami Ishibashi, Constituents of *Amoora cucullata* with TRAIL resistance-overcoming activity, *Organic & Biomolecular Chemistry*, 8, 16, (2010), 3696–3703
<https://doi.org/10.1039/C004927A>
- [15] Robert A. DeFilipps, Gary A. Krupnick, The medicinal plants of Myanmar, *PhytoKeys*, 102, (2018), 1–341
<https://doi.org/10.3897/phytokeys.102.24380>
- [16] Parinuch Chumkaew, Shigeru Kato, Kan Chantrapromma, Potent cytotoxic rocaglamide derivatives from the fruits of *Amoora cucullata*, *Chemical and Pharmaceutical Bulletin*, 54, 9, (2006), 1344–1346
<https://doi.org/10.1248/cpb.54.1344>
- [17] Ni Putu Ermi Hikmawanti, Sofia Fatmawati, Anindita Wulan Asri, The effect of ethanol concentrations as the extraction solvent on antioxidant activity of Katuk (*Sauropus androgynus* (L.) Merr.) leaves extracts, *IOP Conference Series: Earth and Environmental Science*, 2021
<https://doi.org/10.1088/1755-1315/755/1/012060>
- [18] Kindi Farabi, Desi Harneti, Maharani R. Nurlelasari, A. C. Hidayat, Unang Supratman, Khalijah Awang, Yoshihito Shiono, Cytotoxic steroids from the bark of *Aglaia argentea* (Meliaceae), *Chiang Mai University Journal of Natural Sciences*, 16, 4, (2017), 293–306
<https://doi.org/10.12982/CMUJNS.2017.0024>
- [19] Aprilia Permata Sari, Nurlelasari, Azmi Azhari, Desi Harneti, Rani Maharani, Tri Mayanti, Kindi Farabi, Darwati, Unang Supratman, Sofa Fajriah, Mohamad Nurul Azmi, Yoshihito Shiono, New Ergostane-Type Sterol Produced by an Endophytic Fungus *Fusarium phaseoli* Isolated from *Chisocheton macrophyllus* (Meliaceae), *Records of Natural Products*, 16, 6, (2022), 614–621
<http://doi.org/10.25135/rnp.334.2203.2387>
- [20] Isil Gazioglu, Sevcan Semen, Ozden Ozgun Acar, Ufuk Kolak, Alaattin Sen, Gulacti Topcu, Triterpenoids and steroids isolated from Anatolian *Capparis ovata* and their activity on the expression of inflammatory cytokines, *Pharmaceutical Biology*, 58, 1, (2020), 925–931
<https://doi.org/10.1080/13880209.2020.1814356>
- [21] Leslie D. Field, Alison M. Magill, Hsiu Liao Li, *Instructor's Guide and Solutions Manual to Organic Structures from 2D NMR Spectra*, John Wiley & Sons, 2015,